Estimation of soil erosion and sediment yield using GIS

MANOJ K. JAIN

National Institute of Hydrology, Jal Vigyan Bhawan, Roorkee 247 667 (UP), India e-mail: mkj@cc.nih.ernet.in

UMESH C. KOTHYARI

Department of Civil Engineering, University of Roorkee, Roorkee 247 667 (UP), India

Abstract A Geographical Information System (GIS) based method is proposed and demonstrated for the identification of sediment source areas and the prediction of storm sediment yield from catchments. Data from the Nagwa and Karso catchments in Bihar (India) have been used. The Integrated Land and Water Information System (ILWIS) GIS package has been used for carrying out geographic analyses. An Earth Resources Data Analysis System (ERDAS) Imagine image processor has been used for the digital analysis of satellite data for deriving the land cover and soil characteristics of the catchments. The catchments were discretized into hydrologically homogeneous grid cells to capture the catchment heterogeneity. The cells thus formed were then differentiated into cells of overland flow regions and cells of channel flow regions based on the magnitude of their flow accumulation areas. The gross soil erosion in each cell was calculated using the Universal Soil Loss Equation (USLE) by carefully determining its various parameters. The concept of sediment delivery ratio (SDR) was used for determination of the total sediment yield of each catchment during isolated storm events.

Estimation de l'érosion du sol et de l'exportation de sédiments utilisant un SIG

Résumé Une méthode fondée sur l'utilisation d'un système d'information géographique (SIG) est proposée et expérimentée afin d'identifier l'origine des sédiments et de prévoir leur exportation à l'exutoire des bassins lors d'évènements pluvieux. Des données des bassins de Nagwa et de Karso dans l'état du Bihar (Inde) ont été utilisées. Le SIG ILWIS (Integrated Land and Water Information System), système intégré d'informations sur la terre et les eaux a été utilisé pour mener les analyses géographiques. Le logiciel de traitement d'image ERDAS (Éarth Resources Data Analysis System—Système d'analyse de données sur les ressources terrestres), a été utilisé pour l'analyse digitale de données satellitaires en vue de déterminer l'occupation et les caractéristiques des sols des bassins étudiés. Ces bassins ont été discrétisés selon un maillage dont les mailles sont hydrologiquement homogènes afin de représenter l'hétérogénéité des bassins. On a alors distingué les mailles des régions de ruissellement de surface et les mailles d'écoulement en chenaux selon l'importance de leur surface d'alimentation. L'érosion brute du sol dans chaque maille a été calculée en utilisant l'équation universelle des pertes en sol (Universal Soil Loss Equation—USLE) en déterminant soigneusement ses divers paramètres. Le concept de rapport de fourniture de sédiments (Sediment Delivery Ratio-SDR) a été utilisé pour la détermination de l'exportation totale des sédiments de chaque bassin durant des épisodes pluvieux particuliers.

INTRODUCTION

Soil erosion is one of the most critical environmental hazards of modern times. Vast areas of land now being cultivated may be rendered economically unproductive if the

erosion of soil continues unabated. The information on sources of sediment yield within a catchment can be used as a perspective on the rate of soil erosion occurring within that catchment. The process of soil erosion involves detachment, transport and subsequent deposition (Meyer & Wischmeier, 1969). Sediment is detached from the soil surface both by raindrop impact and by the shearing force of flowing water. The detached sediment is transported downslope primarily by flowing water, although there is also a small amount of downslope transport by raindrop splash (Walling, 1988). Once runoff starts over the surface areas and in the streams, the quantity and size of material transported increases with the velocity of the runoff. At some point, the slope may decrease, resulting in a decreased velocity and hence a decreased transport capacity (Haan *et al.*, 1994). The sediment is then deposited, starting with the large primary particles and aggregates. Smaller particles are transported further downslope, resulting in the enrichment of fines. The amount of sediment load passing the outlet of a catchment forms its sediment yield.

Simple methods such as the Universal Soil Loss Equation (USLE) (Musgrave, 1947), the Modified Universal Soil Loss Equation (MUSLE) (Williams, 1975), or the Revised Universal Soil Loss Equation (RUSLE) (Renard et al., 1991b) are frequently used for the estimation of surface erosion and sediment yield from catchment areas (Ferro & Minacapilli 1995; Ferro 1997; Kothyari & Jain, 1997; Ferro et al., 1998; Stefano et al., 1999). Both of these quantities are found to have large variability due to the spatial variation of rainfall and to catchment heterogeneity. Such variability has promoted the use of data intensive process-based distributed models for the estimation of catchment erosion and sediment yield viz. by discretizing a catchment into sub-areas each having approximately homogeneous characteristics and uniform rainfall distribution (Young et al., 1987; Wicks & Bathurst, 1996). The use of Geographical Information System (GIS) methodology is well suited for the quantification of heterogeneity in the topographic and drainage features of a catchment (Shamsi, 1996; Rodda et al., 1999). The objectives of this research were to use GIS for the discretization of the catchments into small grid cells and for the computation of such physical characteristics of these cells as slope, land use and soil type, all of which affect the processes of soil erosion and deposition in the different sub-areas of a catchment. Further GIS methods are also used to partition the sub-areas into overland and channel types, to estimate the soil erosion in individual grid cells and to determine the catchment sediment yield by using the concept of sediment delivery ratio.

METHODOLOGY

Apart from rainfall and runoff, the rate of soil erosion from an area is also strongly dependent upon its soil, vegetation and topographic characteristics. In real situations, these characteristics are found to vary greatly within the various sub-areas of a catchment. A catchment therefore needs to be discretized into smaller homogeneous units before making computations for soil loss. A grid-based discretization is found to be the most reasonable procedure in both process-based models as well as in other simple models (Beven, 1996; Kothyari & Jain, 1997). For the present study, a grid-based discretization procedure was adopted. The cell size to be used for discretization should be small enough so that a grid cell encompasses a hydrologically homogeneous area. Grids thus formed can be categorized as having cells lying on overland areas and

those lying in channel areas. Such a differentiation is necessary because the processes of sediment erosion and delivery in them are widely different (Atkinson, 1995). In the present study such a differentiation was achieved by following the procedure of the channel initiation threshold given in ESRI (1994). In this procedure, a grid cell is considered to lie in an overland region if the size of the area from which it receives a flow contribution is smaller than or equal to a specified threshold area for the initiation of a channel. Cells receiving a flow contribution from an area of more than the threshold value are considered to form the channel grid cells. Cells with no flow accumulation lie on the catchment boundary. Different values of the channel initiation threshold would result in stream networks with different total stream lengths, and consequently, with different drainage densities (Wang & Yin, 1998).

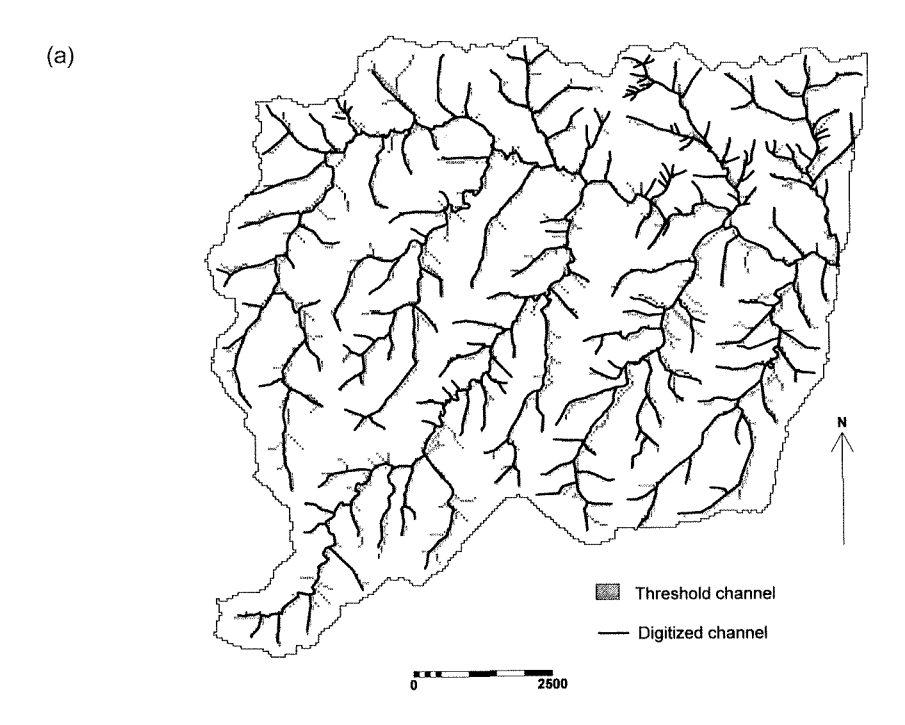
Since the purpose of differentiating grid cells into overland and channel cells is to simulate a catchment as it exists in nature, it is wise to devise some criterion for choosing the value of the threshold area judiciously. Accordingly it was considered that the total stream length generated using a given threshold and the observed total stream length estimated from a 1:25 000 scale topographic map (digitized in vector form) should be the same if the value of the threshold were chosen correctly. Various values of the channel initiation threshold area were tried and for each the length of the generated channel network was compared with the vector digitized channel network length. It was observed that a channel initiation threshold area of 5 ha gave a good reproduction of the observed channel network. It should be noted here that the threshold area is an average indicator and that various physiographic regions may have different thresholds for channel initiation. However, for the catchments under study, an average value is considered to be reasonably representative. The generated channel network and the digitized channel network for the Nagwa and Karso catchments are shown in Fig. 1. As can be seen, the simulated channel network with the average channel initiation threshold value gave a close match to the observed channel network digitized at a 1:25 000 scale for both catchments.

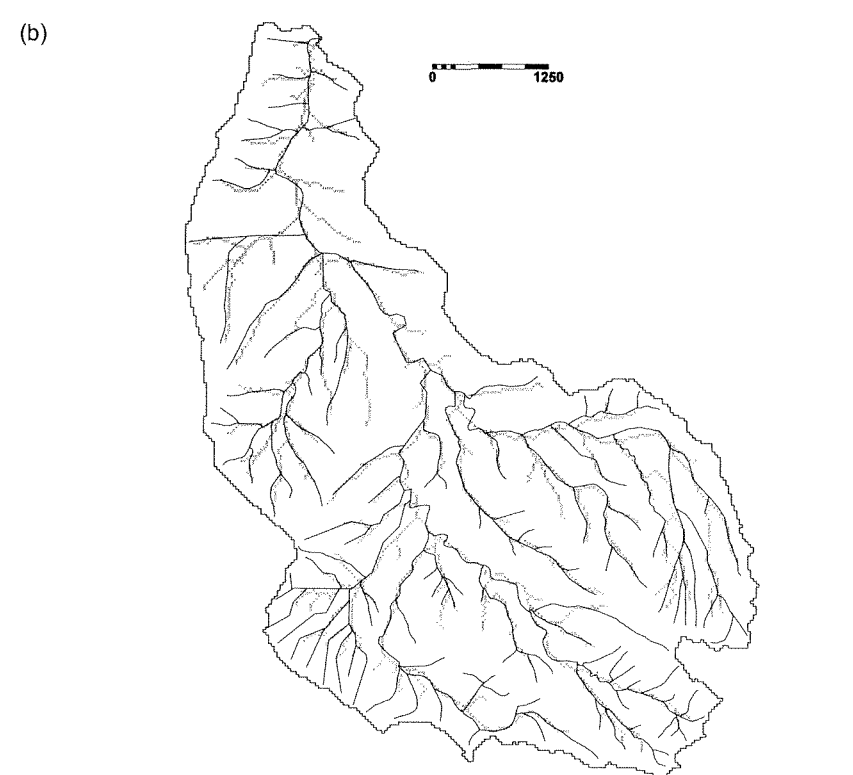
Methods such as the USLE have been found to produce realistic estimates of surface erosion over areas of small size (Wischmeier & Smith, 1978). Therefore, soil erosion within a grid cell was estimated via the USLE. The USLE is expressed as:

$$S_{E} = R \cdot K \cdot LS \cdot C \cdot P \tag{1}$$

where S_{E_i} is the gross amount of soil erosion (t ha⁻¹); R is the rainfall erosivity factor (MJ mm ha⁻¹ h⁻¹); K is the soil erodibility factor (t ha h ha⁻¹ MJ⁻¹ mm⁻¹); LS is the slope steepness and length factor (dimensionless); C is the cover management factor (dimensionless) and P is the supporting practice factor (dimensionless). [Note about units: while ha and ha⁻¹ appear to cancel each other out using conventional arithmetic, these are the units used according to Renard et al., 1991a.]

Values of the factor R of the USLE, as computed by the method of Wischmeier & Smith (1958) and Wischmeier (1959) are applicable for annual values of erosion and do not apply to individual storm events. Cooley (1980) first developed a method for determining R values for individual storm events. Subsequently Renard $et\ al.$ (1991a) proposed a method for computing R values for individual storm events by making use of the unit energy relationship proposed by Brown & Foster (1987). Renard $et\ al.$ (1991a) also proposed that R values for the estimation of annual soil loss be determined by obtaining the long-term average of the R values computed for individual





 $\label{eq:Fig. 1} \textbf{Fig. 1} \ \mbox{Observed and generated channel network (a) for the Nagwa catchment, and (b) for the Karso catchment.}$

storm events. In the present study, the method of Brown & Foster (1987) and Renard et al. (1991a) was used for computing R values for individual storm events.

For computation of the *LS* factor in a grid cell, a minimum cell area of about 0.01 km² is required in order to have a representative estimate of its *LS* factor for use in the USLE (Wischmeier & Smith, 1978; Panuska *et al.*, 1991). With this area the maximum permissible length is 141 m (Panuska *et al.*, 1991). However, a cell size smaller than this is to be used for soil loss estimation using GIS. Moore & Burch (1986) and Moore & Wilson (1992) derived an equation based on unit stream power theory for estimating the *LS* factor in cells smaller than the plots of Wischmeier & Smith (1978). The *LS* factor in the present study was therefore computed for overland cells by using the equation stated by Moore & Wilson (1992):

$$LS = \left[\frac{A_s}{22.13} \right]^n \cdot \left[\frac{\sin \beta}{0.0896} \right]^m \tag{2}$$

where A_s is the specific area (=A/b), defined as the upslope contributing area for an overland cell (A) per unit width normal to the flow direction (b); β is the slope gradient in degrees; n = 0.4; and m = 1.3. For channel grid cells, the value of A is considered to be equal to the value of the threshold area corresponding to channel initiation. The use of equation (2) in the estimation of the LS factor allows the introduction of the three-dimensional hydrological and topographic effects of converging and diverging terrain on soil erosion (Panuska $et\ al.$, 1991).

The values for the factors K, C and P were estimated for different grids in overland and channel regions as per Wischmeier & Smith (1978) using the classified satellite data for land cover and soil. The study catchments were covered by the satellites Landsat TM (path 140 and row 43 on 7 May 1991) and IRS 1C LISS-III (path 105 and row 55 on 28 November 1996). The areas of interest were first cut from the entire path/row of the LANDSAT TM and IRS 1C LISS-III scenes and were geo-coded using the method suggested by Sabins (1997) at 30 and 24 m pixel resolutions, respectively, by means of the Earth Resources Data Analysis System (ERDAS) Imagine image processing software (ERDAS, 1998). The geo-coded scenes were then masked by the boundaries of the catchments derived earlier for delineating the areas lying within the catchment. Land cover and soil maps were then generated using the supervised classification scheme (Sabins, 1997) using TM data. The IRS 1C LISS-III data were used only to clarify confusing pixels as to the class in which they belonged. In the Nagwa catchment, four types of land cover viz. agriculture (small grain), fairly dense forest, open scrub and wasteland, were identified and mapped. Similarly, in the Karso catchment, three land cover categories viz. agriculture (mainly paddy), fairly dense forest and open scrub were identified and mapped. Land cover information was thus available for each cell of both catchments. Based on land cover categories, the attribute values for the C factor were assigned to individual cells from the tabulated values of Wischmeier & Smith (1978). Table 1 summarizes the land cover statistics and the C factors used for the Nagwa and Karso catchments. The P factor was taken equal to 0.3 for all land cover categories for both catchments as reported by Kothyari et al. (1996) for these catchments.

Soil types could not be evaluated directly from Landsat TM images. However, based on morphological features, Landsat tonal variations and associated soil texture,

Table 1	Land	cover statistics	for the	catchments studied.
---------	------	------------------	---------	---------------------

Catchment	Land cover	Area (km²)	C factor	a value
Nagwa:				
	Fairly dense forest	5.55	0.003	0.76
	Open scrub	8.32	0.040	1.55
	Agriculture (small grain)	59.18	0.290	2.62
	Waste land	19.41	0.400	3.08
Karso:				
	Fairly dense forest	9.77	0.003	0.76
	Open scrub	1.40	0.040	1.55
	Agriculture (mainly paddy)	16.76	0.260	1.55

Table 2 Soil type statistics for the catchments studied.

Catchment	Soil type	Area (km²)	K factor (t ha h ha ⁻¹ MJ ⁻¹ mm ⁻¹)
Nagwa:			
	Clay loam	5.86	0.042
	Very fine sandy loam	17.00	0.049
	Sandy loam	69.60	0.057
Karso:			
	Loamy sand	5.47	0.032
	Clay loam	8.44	0.042
	Silty clay	14.02	0.037

and limited ground truth data, different soil types were distinguished, classified and mapped in the study catchments. The soils were classified into three categories viz. clay loam, very fine sandy loam and sandy loam in the Nagwa catchment and loamy sand, clay loam and silty clay loam in the Karso catchment. The soil characteristics such as fraction of sand, silt, clay and organic matter and other related parameters for the mapped soil categories were taken from SWCD (1991) for both catchments. Thus the information on soil type in individual grids of both catchments was known. The parameter K values for the mapped soil categories were then estimated for each of the cells using the procedure given in the nomograph of Wischmeier & Smith (1978). The estimated K values for the mapped soil units of the Nagwa and Karso catchments are given in Table 2.

Use of equation (1) produced the estimates of gross soil erosion in the overland region and channel region of each catchment. The gross amount of soil erosion for each cell during a storm event was generated by multiplying the term *KLSCP* with the *R* factor for the corresponding storm event given in Table 3. The eroded sediment was routed from each cell to the catchment outlet using the concept of sediment delivery ratio described below.

Sediment delivery ratio

In a catchment, part of the soil eroded in an overland region deposits within the catchment before reaching its outlet. The ratio of sediment yield to total surface

Date of event	R value	Sediment yield	Ratio	
	$(MJ mm ha^{-1} h^{-1})$	Observed	Computed	Obs./Comp.
Nagwa catchment.	•			
6 July 1989	533.06	2172.81	4747.15	0.45
20 July 1989	574.99	7143.23	5128.01	1.39
28 July 1989	419.60	3246.84	3719.04	0.87
Karso catchment:				
3 August 1991	110.82	112.35	135.44	0.83
4 August 1991	182.13	156.21	252.50	0.62
17 August 1991	30.10	287.61	24.50	11.74
27 August 1991	144.85	117.95	189.96	0.62
28 August 1991	116.61	283.63	145.17	1.95

Table 3 Computed and observed values of sediment yield.

erosion is termed the sediment delivery ratio (D_R) . Values of D_R for an area are found to be affected by catchment physiography, sediment sources, transport system, texture of eroded material, land cover etc. (Walling, 1983, 1988; Richard, 1993). However, variables such as catchment area, land slope and land cover have been mainly used as parameters in empirical equations for D_R (Hadley *et al.*, 1985; Maner, 1958; Roehl, 1962; Williams & Berndt, 1972; Kothyari & Jain, 1997).

Ferro & Minacapilli (1995) and Ferro (1997) hypothesized that D_R in grid cells is a strong function of the travel time of overland flow within the cell. The travel time is strongly dependent on the topographic and land cover characteristics of an area and therefore its relationship with D_R is justified. Based on their studies, the following empirical relationship was assumed herein for a grid cell lying in an overland region of a catchment:

$$D_{R_i} = \exp(-\gamma t_i) \tag{3}$$

where t_i is the travel time (h) of overland flow from the *i*th overland grid to the nearest channel grid down the drainage path and γ is a coefficient considered as constant for a given catchment.

The travel time for grids located in a flow path to the nearest channel can be estimated if one knows the lengths and velocities for the flow paths. In grid-based GIS analysis, the direction of flow from one cell to a neighbouring cell is ascertained by using an eight direction pour point algorithm (ESRI, 1994). This algorithm chooses the direction of steepest descent among the eight permitted choices. Once the pour point algorithm identifies the flow direction in each cell, a cell-to-cell flow path is determined to the nearest stream channel and thus to the catchment outlet (Maidment, 1994). If the flow path from cell i to the nearest channel cell traverses m cells and the flow length of the ith cell is l_i (which can be equal to the length of a square side or to a diagonal depending on the direction of flow in the ith cell) and the velocity of flow in cell i is v_i , the travel time t_i from cell i to the nearest channel can be estimated by summing the time through each of the m cells located in that flow path:

$$t_i = \sum_{i=1}^m \frac{l_i}{v_i} \tag{4}$$

For the present study, the method for the determination of the overland flow velocity proposed by the US Soil Conservation Service was chosen due to its simplicity and to the availability of the information required (SCS, 1975). The flow velocity is considered to be a function of the land surface slope and the land cover characteristics:

$$v_i = a_i S_i^b \tag{5}$$

where b is a numerical constant equal to 0.5 (SCS, 1975; Ferro & Minacapilli, 1995), S_i is the slope of the ith cell and a_i is a coefficient related to land use (Haan et al. 1994). Introducing equations (4) and (5) into equation (3) gives:

$$D_{R_i} = \exp\left(-\gamma \sum_{i=1}^m \frac{l_i}{a_i S_i^{0.5}}\right) \tag{6}$$

Note that $l_i/S_i^{0.5}$ is the definition of travel time used by Ferro & Minacapilli (1995). Values of the coefficient a_i for different land uses were adopted from Haan (1994) and those are listed in Table 1 for both the Nagwa and Karso catchments. High spatial variation in the a_i values for the cases studied may be noted.

If S_{E_i} is the amount of soil erosion produced within the *i*th cell of the catchment estimated using equation (1), then the sediment yield for the catchment, S_y , during a storm event was obtained as below (Kothyari & Jain, 1997):

$$S_{y} = \sum_{i=1}^{N} D_{R_{i}} S_{E_{i}} \tag{7}$$

where N is the total number of cells over the catchment and the term D_{R_i} is the fraction of S_{E_i} that ultimately reaches the nearest channel. Since the D_{R_i} of a cell is hypothesized as a function of travel time to the nearest channel, it implies that the gross erosion in that cell multiplied by the D_{R_i} value of the cell becomes the sediment yield contribution of that cell to the nearest stream channel. The D_{R_i} values for the cells marked as channel cells are assumed to be unity. This hypothesis is accurate at the event scale only if the catchment is small while it is applicable at the mean annual scale in other cases according to Playfair's law (Boyce, 1975).

HYDROLOGICAL DATA

The data used in this study are those from the catchments of Nagwa (23°59′33″N–24°05′37″N; 85°16′41″E–85°23′50″E) and Karso (24°16′47″N–24°12′18″N; 85°24′20″E–85°28′06″E) in Bihar, India (Kothyari *et al.*, 1996). Some of the hydroclimatic conditions of the catchments are described in Table 4. The data used for these catchments included the variation of rainfall, runoff, and sediment yield with time, topographic details, soil types and land cover patterns. In these catchments the rainfall was measured using single recording raingauges located at the outlet of each catchment. Automatic water level recorders were used to measure the stream stage and runoff was

Catchment	Area (km²)	Av. land slope (%)	Av. annual precipitation (mm)	Land cover * (%)	Dates of the selected storm events
Karso Barakar catchment, Bihar (India)	27.93	7.3	1243	AG = 60 FO = 35 OS = 5	3 August 1991 28 July 1991 27 July 1991 4 August 1991 17 August 1991
Nagwa Damodar catchment, Bihar (India)	92.46	1.3	1076	AG = 64 FO = 6 OS = 9 WL = 21	6 July 1989 20 July 1989 28 July 1989

Table 4 Hydroclimatic data for the selected catchments.

derived using the relevant rating curve. Sediment yield was determined using a Coshocton wheel silt sampler during low flow periods. During the periods of moderate and high flows, the sampling for sediment yield was done using bottle samplers. The bottle sampler is a point integrating sampler designed to collect a sample, which yields the mean concentration of the suspended sediment load at any desired point in a vertical (Garde & Raju, 1985). Samples of the suspended sediment collected through bottle sampler were subsequently filtered, dried and weighed in the laboratory for the determination of the sediment load. Thus the sediment yield as estimated in the present study represents only the total suspended load transported by the stream to its outlet. Bed contact and saltation loads were not accounted for. Values of the USLE parameters for the grid cells of the catchments were derived using the procedures discussed previously. The dates of storm events studied are given in Table 4.

ANALYSIS AND DISCUSSION OF RESULTS

Generation of digital input maps

The river network and contour map of the study areas were digitized using the Integrated Land and Water Information System, ILWIS (ITC, 1998) from Survey of India maps at a scale of 1:25 000. The digitized segment contour maps were then interpolated at 50-m and 30-m grid cells by using ILWIS to generate Digital Elevation Models (DEM) of the Nagwa and Karso catchments. These DEMs were further analysed to remove pits and flat areas to maintain continuity of flow to the catchment outlets. The corrected DEMs were next used to delineate the catchment boundaries of the catchments using an eight direction pour point algorithm (ESRI, 1994). The DEMs were then further analysed to distinguish overland and channel cells.

To distinguish between overland and channel cells in each catchment, the flow direction and the flow accumulation in the cells were calculated. The flow direction in any of the eight directions (four sides and four diagonals) was determined by using the pour point algorithm (ESRI, 1994). The flow accumulation, which denotes the accumulated up-slope contributing area for a given cell, was calculated by summing the cell areas of all up-slope cells draining into it.

^{*} AG = agriculture; FO = forest; OS = open scrub; WL = waste land.

Generation of the erosion potential map

Maps for values of the USLE parameters viz. *K*, *LS*, *C* and *P*, were overlaid to form a combined map of the composite term *KLSCP*. The storm events selected for the study of the Karso catchment occurred between 27 July and 18 August 1991, while those in the Nagwa catchment occurred between 6 July and 28 July 1989. Changes occurring in the values of the factor *C* due to crop growth over such small duration were neglected. The composite term *KLSCP* represents the soil erosion potential of different grid cells. A high value of this term indicates a higher potential of soil erosion in the cell and *vice versa*. Figure 2 shows the maps indicating areas of varying *KLSCP* values and hence the soil erosion potential in the different segments of the of Nagwa and Karso catchments. The information shown in Fig. 2 may also be used for the identification of the sediment source areas of the catchments.

Sediment delivery ratio

The sensitivity of the coefficient γ appearing in equation (3) for D_R was studied empirically. The value of γ was varied between 0.1 and 1.6 with an increment of 0.1 and the S_y value was computed for each storm event in both the catchments by using equations (3) and (6). However, the computed values of S_y were found not to be very sensitive to the value of γ used in equation (3). This variation in the computed values of S_y was not more than 10% in any of the storm events for a large range of γ values. Therefore, for simplicity, γ equal to unity was assumed. Figure 3 shows generated maps of D_R values for the Nagwa and Karso catchments. It can be seen from this figure that, as expected, large D_R values are associated with steep headwater areas, while channel areas in the catchment and smaller D_R values are mainly found to be associated with the overland regions that surround the confluences of the main stream with the smaller order streams.

Computations for soil erosion and sediment yield

Figure 4(a) and (b) shows the gross soil erosion during the storm event of 28 July 1989 for the Nagwa catchment for the storm event of 3 August 1991 for the Karso catchment, respectively. Comparisons between observed and computed sediment yields for two different storm events are given in Table 3. As can be seen, the method described herein produced estimates of sediment yield with reasonable accuracy. Note that the coefficient values used in the various equations were determined using standard procedures and without any calibration. The prediction accuracy of the proposed methodology can be rated as satisfactory, particularly considering the fact that such prediction from some of the process-based models show large differences between measured and computed sediment yields (Wu et al., 1993). Nevertheless, poor agreement is found to exist between the observed and computed values of sediment yield for one storm event in each of the Karso and Nagwa catchments (see Table 3). These errors are ascribed to the likely uncertainties due to the possibly poor representativeness of the single raingauge used for measuring catchment rainfall. The

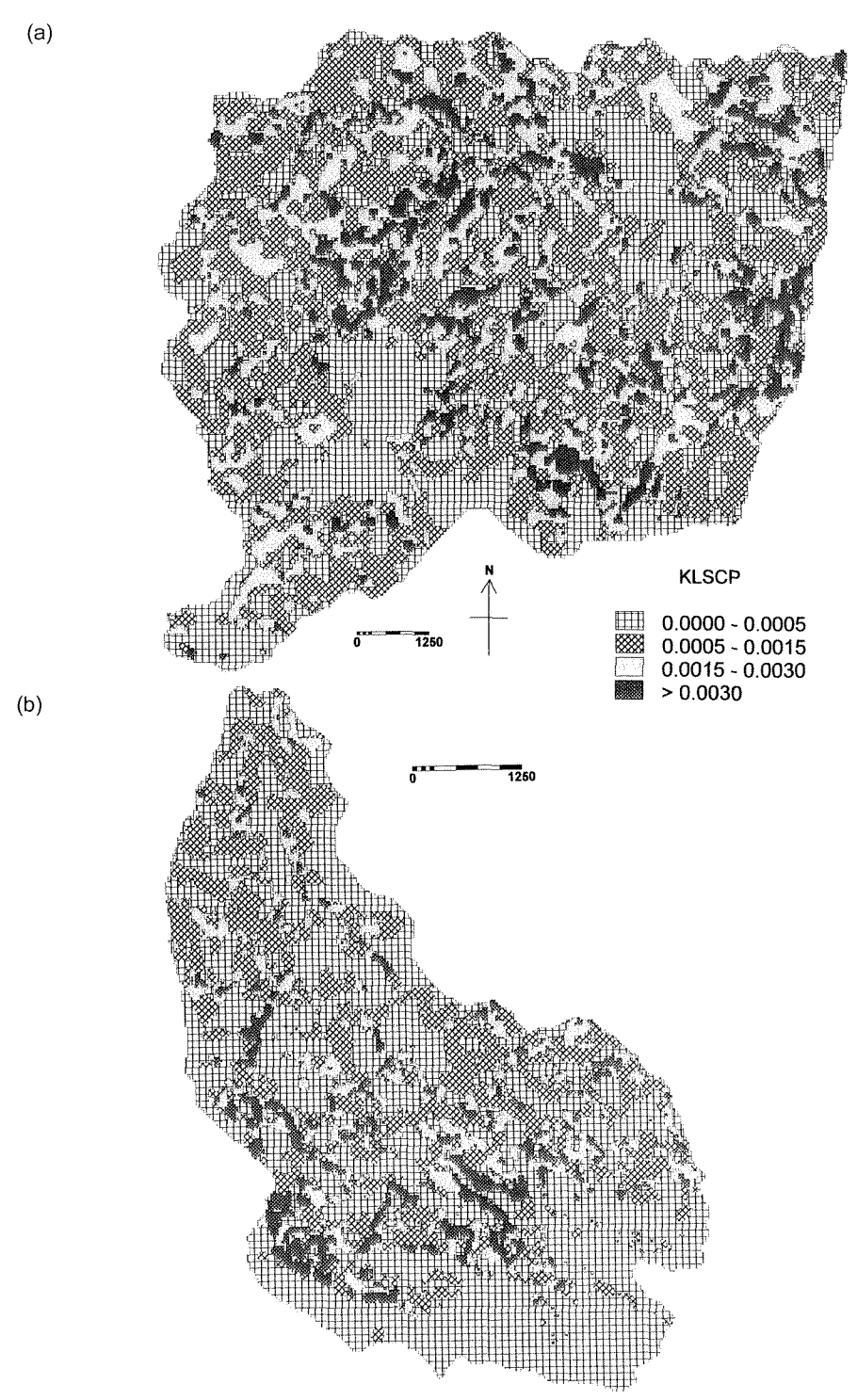
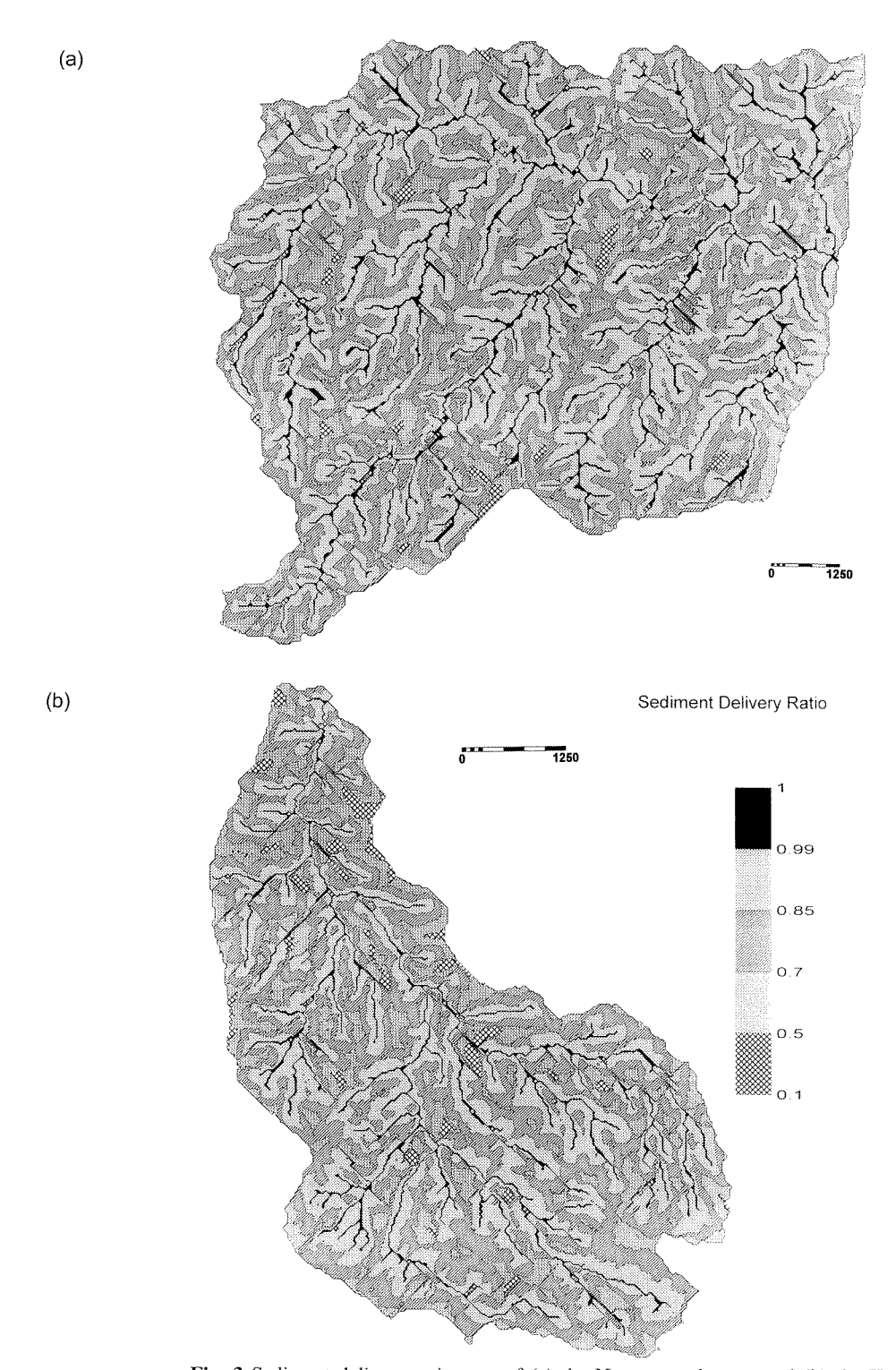


Fig. 2 Soil erosion potential maps of (a) the Nagwa catchment, and (b) the Karso catchment.



 ${\bf Fig.~3}$ Sediment delivery ratio map of (a) the Nagwa catchment, and (b) the Karso catchment.

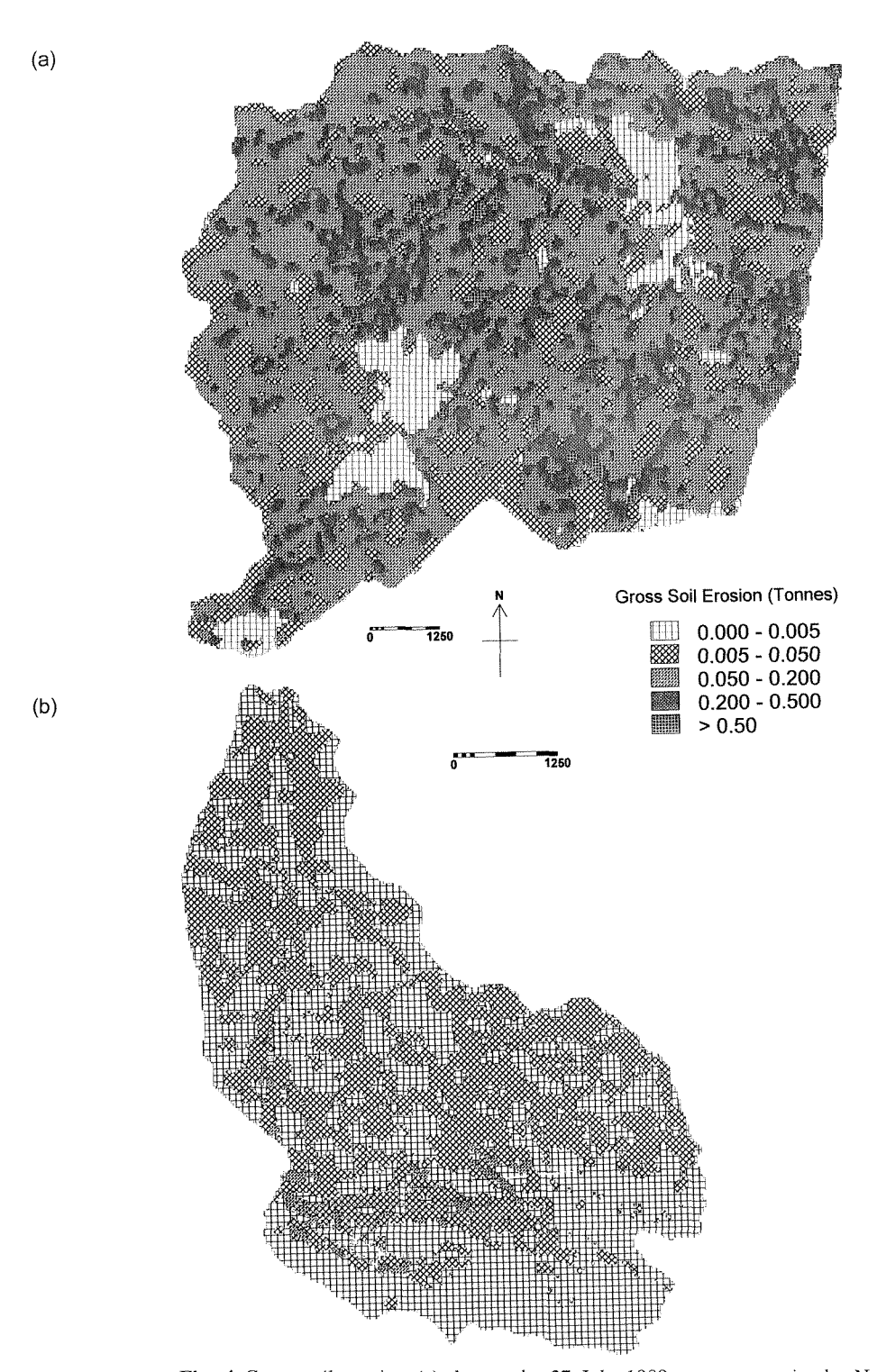
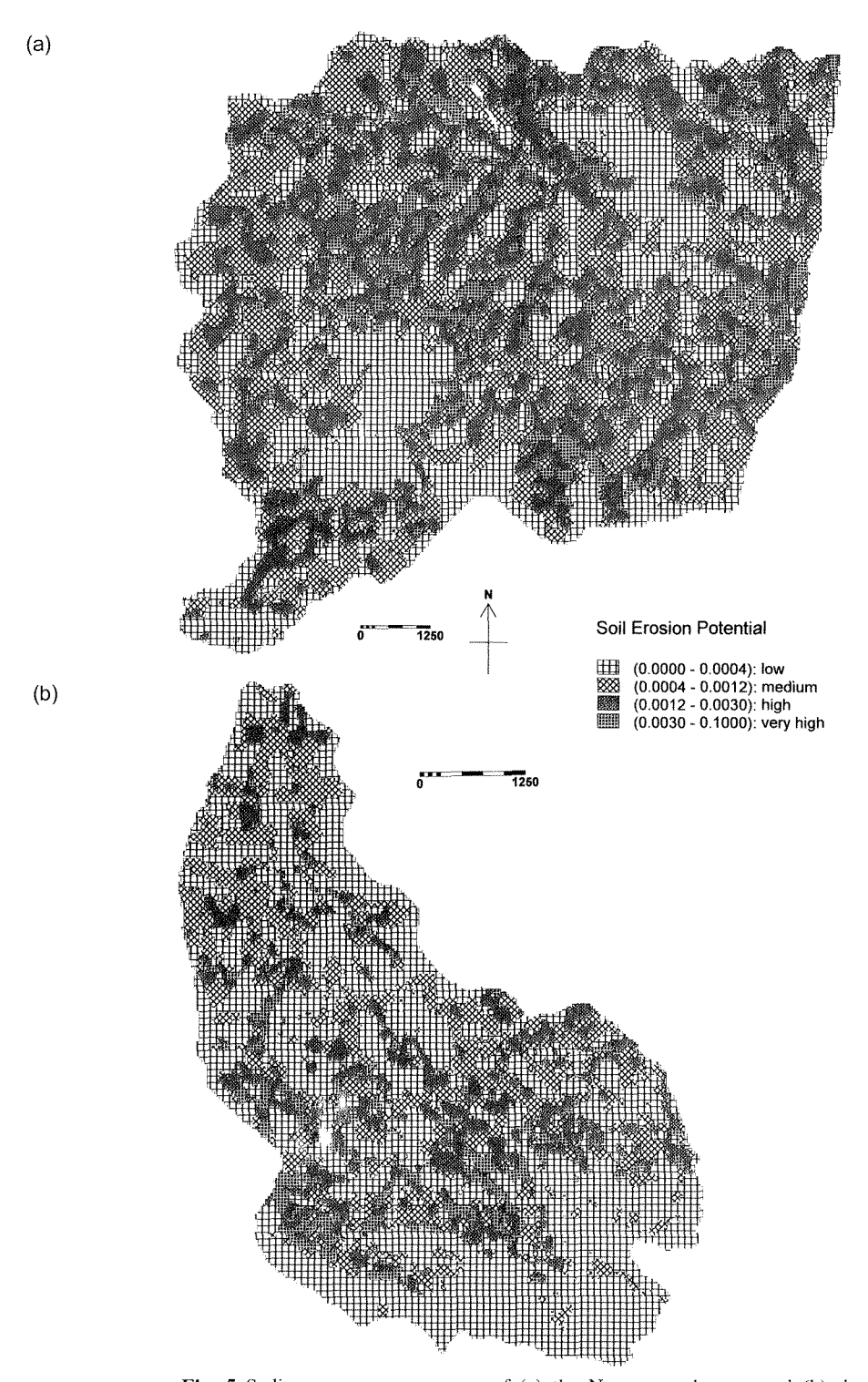


Fig. 4 Gross soil erosion (a) due to the 27 July 1989 storm event in the Nagwa catchment, and (b) due to the 3 August 1991 storm event in the Karso catchment.



 $\boldsymbol{Fig.\ 5}$ Sediment source area map of (a) the Nagwa catchment, and (b) the Karso catchment.

assumption of constant *KLSCP* for the catchment may be considered to be another source of uncertainty.

Identification of sediment source areas

The gross soil erosion map and sediment delivery ratio maps were overlaid in ILWIS to identify the source areas for sediments reaching the outlet from within each catchment. Through such overlaying, the areas producing large sediment amounts in the catchments have been identified and are shown in Fig. 5(a) and (b) for the Nagwa and Karso catchments, respectively. It is to be emphasized that the areas producing more sediment would need special priority for the implementation of soil erosion control measures.

CONCLUSIONS

A GIS-based methodology has been proposed and validated for the identification of sediment source areas and prediction of storm sediment yield from catchment areas. The ILWIS GIS was used for discretizing the catchments into grid cells and the ERDAS Imagine image processor used for processing satellite data related to land cover and soil characteristics. Grid cell drainage directions and catchment boundaries were generated by forming the DEM using a pour point model. The DEM was further analysed to classify grid cells into overland region cells and channel region cells by using the concept of a channel initiation threshold area.

After assigning values to the various parameters of the USLE in individual cells, their gross surface erosion was calculated. The sediment delivery ratio of a cell in the overland flow region was hypothesized to be a function of the travel time of overland flow from the given cell to the nearest downstream channel cell. For channel cells, the sediment delivery ratio was assumed to be unity. Reasonable results were obtained for storm sediment yields on the Nagwa and Karso catchments by using the proposed method.

Acknowledgements The authors wish to thank sincerely the anonymous reviewers whose comments greatly improved the quality of the paper.

REFERENCES

Atkinson, E. (1995) Methods for assessing sediment delivery in river systems. Hydrol. Sci. J. 40(2), 273–280.

Beven, K. J. (1996) A discussion of distributed modelling. In: *Distributed Hydrological Modelling* (ed. by M. B. Abbott & J. C. Refsgaard), 255–278. Kluwer, Dordrecht, The Netherlands.

Boyce, R. C. (1975) Sediment routing with sediment delivery ratios. In: Present and Prospective Technology for Predicting Sediment Yields and Sources, 61–65. US Dept. Agric. Publ. ARS-S-40.

Brown, L. C. & Foster, G. R. (1987) Storm erosivity using idealized intensity distributions. *Trans. Am. Soc. Agric. Engrs* 30(2), 379–386.

Cooley, K. R. (1980) Erosivity values for individual design storms. J. Irrig. Drain. Div. ASCE 106(IR2), 135–145.

Di Stefano, C., Ferro, V. & Porto, P. (1999) Modelling sediment delivery process by a stream tube approach. *Hydrol. Sci. J.* **44**(5), 725–742.

ERDAS (Earth Resources Data Analysis System) (1998) ERDAS Imagine 8.3.1. ERDAS Inc., Atlanta, Georgia, USA.

ESRI (Environmental Systems Research Institute) (1994) Cell based modelling with GRID. Environmental Systems Research Institute Inc., Redlands, California, USA.

Ferro, V. (1997) Further remarks on a distributed approach to sediment delivery. Hydrol. Sci. J. 42(5), 633-647.

- Ferro, V. & Minacapilli, M. (1995) Sediment delivery processes at basin scale. Hydrol. Sci. J. 40(6), 703-717.
- Ferro, V., Porto, P. & Tusa, G. (1998) Testing a distributed approach for modelling sediment delivery. *Hydrol. Sci. J.* 43(3), 425-442.
- Garde, R. J. & Raju, K. G. (1985) Mechanics of Sediment Transportation and Alluvial Stream Problems. Wiley Eastern Limited, New Delhi, India.
- Haan, C. T., Barfield, B. J. & Hayes, J. C. (1994) Design Hydrology and Sedimentology for Small Catchments. Academic Press, New York.
- Hadley, R. F., Lal, R., Onstad, C. A., Walling, D. E. & Yair, A. (1985) Recent Developments in Erosion and Sediment Yield Studies. UNESCO (IHP) Publication, Paris, France.
- ITC (International Institute for Aerospace Survey and Earth Sciences) (1998) The Integrated Land and Water Information System (ILWIS). Int. Inst. for Aerospace Survey and Earth Sciences, Enschede, The Netherlands.
- Kothyari, U. C. & Jain, S. K. (1997) Sediment yield estimation using GIS. Hydrol. Sci. J. 42(6), 833-843.
- Kothyari, U. C., Tiwari, A. K. & Singh, R. (1996) Temporal variation of sediment yield. J. Hydrol. Engng Div. ASCE 1(4), 169-176.
- Maidment, D. R. (1994) Digital delineation of watersheds and stream networks in the Allegheny basin. Prepared for Hydrologic Engineering Centre, Davis, California, USA.
- Maner, S. B. (1958) Factors affecting sediment delivery ratio in the red hill physiographic area. *Trans. AGU* 39(4), 669–675.
- Meyer, L. D. & Wischmeier, W. H. (1969) Mathematical simulation of the processes of soil erosion by water. *Trans. Am. Soc. Agric. Engrs* 12(6), 754–758.
- Moore, I. D. & Burch, G. J. (1986) Physical basis of the length slope factor in the Universal Soil Loss Equation. Soil Sci. Soc. Am. J. 50(5), 1294–1298.
- Moore, I. D. & Wilson, J. P. (1992) Length slope factor for the Revised Universal Soil Loss equation: simplified method of solution. J. Soil Wat. Conserv. 47(5), 423–428.
- Musgrave, G. (1947) The quantitative evaluation of factors in water erosion, a first approximation. *J. Soil Wat. Conserv.* **2**(3), 133–138.
- Panuska, J. C., Moore, I. D. & Kramer, L. A. (1991) Terrain analysis: integration into the agricultural nonpoint source (AGNPS) pollution model. J. Soil Wat. Conserv. 46(1), 59-64.
- Renard, K. G., Foster, G. R., Weesies, G. A. & McCool, D. K. (1991a) Predicting soil erosion by water—a guide to conservation planning with the Revised Universal Soil Loss Equation (RUSLE). Report ARS-703, US Dept Agric., Agricultural Research Service.
- Renard, K. G., Foster, G. R., Weesies, G. A. & Porter, J. P. (1991b) RUSLE, Revised Universal Soil Loss Equation. J. Soil Wat. Conserv. 46(1), 30-33.
- Richard, K. (1993) Sediment delivery and the drainage network. In: *Channel Network Hydrology* (ed. by K. Beven & M. J. Kirkby), 222–254. John Wiley & Sons, Chichester, West Sussex, UK.
- Rodda, H. J. E., Demuth, S. & Shankar, U. (1999) The application of a GIS based decision support system to predict nitrate leaching to ground water in south Germany. *Hydrol. Sci. J.* 44(2), 221–236.
- Roehl, J. W. (1962) Sediment source areas, delivery ratios and influencing morphological factors. In: *Symposium of Bari* (1–8 October 1962), 202–213. IAHS Publ. no. 59.
- Sabins, F. S. (1997) Remote Sensing: Principles and Interpretations (third edn). W.H. Freeman and Company, New York.
- SCS (Soil Conservation Service) (1975) Urban hydrology for small watersheds. Technical release no. 55, Soil Conservation Service, United States Dept of Agric., Washington DC, USA.
- Shamsi, U. M. (1996) Storm-water management implementation through modeling and GIS. J. Wat. Resour. Plan. Manage. ASCE 122(2), 114–127.
- SWCD (Soil and Water Conservation Division) (1991) Evaluation of Hydrological Data (vols I and II), 269. Ministry of Agriculture, Govt of India, New Delhi, India.
- Walling, D. E. (1983) The sediment delivery problem. J. Hydrol. 65, 209-237.
- Walling, D. E. (1988) Erosion and sediment yield research—some recent perspectives. J. Hydrol. 100, 113-141.
- Wang, X. & Yin, Z. Y. (1998) A comparison of drainage networks derived from digital elevation models at two scales. J. Hydrol. 210, 221–241.
- Wicks, J. M. & Bathurst, J. C. (1996) SHESED: A physically based, distributed erosion and sediment yield component for the SHE hydrological modelling system. J. Hydrol. 175, 213–238.
- Wischmeier, W. H. (1959) A rainfall erosion index for a universal soil loss equation. In: *Proc. Soil Sci. Soc. Am.* 23, 246–249.
- Wischmeier, W. H. & Smith, D. D. (1958) Rainfall energy and its relationship to soil loss. Trans. AGU 39(3), 285-291.
- Wischmeier, W. H. & Smith, D. D. (1978) Predicting Rainfall Erosion Losses. Agriculture Handbook no. 537, USDA Science and Education Administration.
- Williams, J. R. (1975) Sediment routing for agricultural watersheds. Wat. Resour. Bull. 11, 965-974.
- Williams, R. & Berndt, H. D. (1972) Sediment yield computed with universal equation. J. Hydraul. Div. ASCE 98(HY12), 2087–2098.
- Wu, T. H., Hall, J. A. & Bonta, J. V. (1993) Evaluation of runoff and erosion models. J. Irrig. Drain. Div. ASCE 119(4), 364-382.
- Young, R. A., Onstad, C. A., Bosch, D. D. & Anderson, W. P. (1987) AGNPS: An agricultural non point source pollution model. Conservation Research Report 35, US Dept. Agric. Res. Services, Washington DC, USA.